ELSEVIER

Catalysis Today 66 (2001) 241–248

CATALYSIS TODAY

www.elsevier.com/locate/cattod

Design and optimisation of a multi-stage bubble column slurry reactor for Fischer–Tropsch synthesis

C. Maretto [a], R. Krishna [b,*]

[a] *Advanced Engineering, EniTecnologie S.p.A., S. Donato, Milan, Italy*

[b] *Department of Chemical Engineering, University of Amsterdam, Nieuwe Achtergracht 166, 1018 WV Amsterdam, The Netherlands*

Abstract

For carrying out the Fischer–Tropsch synthesis of heavy paraffins starting from syngas ($CO + H_2$), a multi-stage bubble column slurry reactor design is carried out. The advantages of this reactor configuration with respect to a conventional slurry reactor design, consisting of one well-mixed stage, are (a) increased syngas conversion, and (b) increased reactor productivity. The multi-stage bubble column construction requires installation of additional cooling surface area in order to keep the exothermic reaction within the desired temperature limits.

Keywords: Bubble columns; Churn-turbulent flow regime; Bubble rise velocity; Multi-stage column; Liquid phase backmixing; Scale up; Fischer–Tropsch reaction

1. Introduction

The Fischer–Tropsch (FT) synthesis process aims to produce middle distillates from natural gas, through three main steps: (1) conversion of natural gas to syngas ($CO + H_2$) by, e.g., catalytic partial oxidation, (2) conversion of syngas to hydrocarbons, mostly paraffins in the range C_5 to C_{100+}, using FT synthesis, and (3) hydrocracking of the paraffinic hydrocarbons to middle distillates. The FT synthesis step (2) is highly exothermic and the bubble column slurry reactor is the ideal reactor choice to this purpose, due to the possibility of achieving near isothermal conditions and also because of the relatively high heat transfer coefficients to cooling tubes [1–8]. In both the commercial scale FT slurry reactor operated by Sasol [9,10] and the Exxon technology reactor under development [11,12], the slurry phase can be considered to be more or less completely backmixed.

The objective of our study is to point out the advantages to use a multi-stage bubble column for the slurry reactor design optimisation, reducing the overall backmixing of the slurry phase, where the FT reaction takes place. Fig. 1 gives a schematic representation of the slurry reactor. Staging of the slurry phase is achieved by introducing sieve plates (or other means), which also act as spacers for the cooling tubes. The results of a detailed design and optimisation study are presented. The reaction kinetics for the FT synthesis reaction is taken from the literature. The hydrodynamics scale-up information are taken from extensive experimental studies carried out at the University of Amsterdam in columns of 0.05, 0.1, 0.15, 0.174, 0.19, 0.38 and 0.63 m diameter with a variety of liquids (water, paraffin oil, tetradecane, Tellus oil) and slurries of different concentrations of silica particles (particle size = 38 μm) in paraffin oil. The details of the hydrodynamics of bubble column slurry

* Corresponding author. Tel.: +31-20-525-7007; fax: +31-20-525-5604.
E-mail address: krishna@its.chem.uva.nl (R. Krishna).

0920-5861/01/$ – see front matter
PII: S0920-5861(00)00626-X

Nomenclature

a	Yates–Satterfield reaction rate constant (mol kg_{cat}^{-1} bar^{-2} s^{-1})
a^*	Yates–Satterfield reaction rate constant (m^6 mol^{-1} m_{slurry}^{-3} s^{-1})
a_w	specific heat exchange surface (m^2 m^{-3})
A	reactor section (m^2)
b	Yates–Satterfield absorption constant (bar^{-1})
b^*	Yates–Satterfield absorption constant (m^3 mol^{-1})
c_G	molar concentration in the gas phase (mol m^{-3})
c_L	molar concentration in the liquid phase (mol m^{-3})
D_L	diffusion coefficient in the liquid phase (m^2 s^{-1})
$D_{L,ref}$	reference diffusion coefficient of N_2 in turpentine-5 (m^2 s^{-1})
D_T	column diameter (m)
Fr	Froude number (–)
H	total dispersion height of the reactor (m)
k_La	volumetric mass transfer coefficient (s^{-1})
m	Henry constant (–)
N	number of stages (–)
p	partial pressure in gas phase (bar)
P	total pressure (bar)
Pr	Prandtl number (–)
R_{CO+H_2}	synthesis gas consumption rate (mol kg_{cat}^{-1} s^{-1})
Re	Reynolds number (–)
St	Stanton number (–)
T	reactor temperature (K)
U	superficial gas velocity (m s^{-1})
U_L	superficial liquid velocity (m s^{-1})
z	axial coordinate (m)

Greek letters

α	contraction factor (–)
ε	total gas holdup (–)
ε_L	liquid phase holdup (–)
μ_{SL}	slurry viscosity (Pa s)
ξ	dimensionless distance along the reactor height (–)
ρ_L	liquid density (kg m^{-3})
ρ_p	particle density (kg $m_{particle}^{-3}$)
ρ_S	solid volumetric concentration in the slurry phase (–)
ρ_{SK}	solid skeleton density (kg m_{solids}^{-3})
ρ_{SL}	slurry density (kg m_{slurry}^{-3})
χ_{CO+H_2}	syngas conversion (–)

Subscripts

CO	referring to CO
H_2	referring to H_2
w	referring to cooling surface wall

Superscripts

inlet	referring to reactor inlet conditions
j	referring to stage j
$*$	referring to equilibrium conditions

reactors have been reported in earlier work carried out at the University of Amsterdam [13–35].

2. Multi-stage slurry reactor concept

The preferred flow regime to operate a commercial slurry bubble column reactor for FT synthesis is the churn-turbulent regime, because of the necessity to deal with very large syngas throughputs and to improve heat transfer to cooling surfaces. The churn-turbulent regime is characterised by a wide distribution of bubble sizes. To describe the hydrodynamics of a slurry bubble column operating in the heterogeneous regime, we adopted the generalised two-phase model [3]. This approach distinguishes a "dilute" phase, i.e. the fraction of gas which flows through the reactor as large bubbles (20–70 mm in size), and a "dense" phase, composed by the liquid phase, the suspended solid particles and the remaining fraction of gas, entrained in the liquid as small bubbles (1–10 mm in size). The total gas holdup, ε, which is an important hydrodynamic parameter affecting reactor performances, is the sum of two contributions: (1) large bubbles, and (2) small bubbles, and

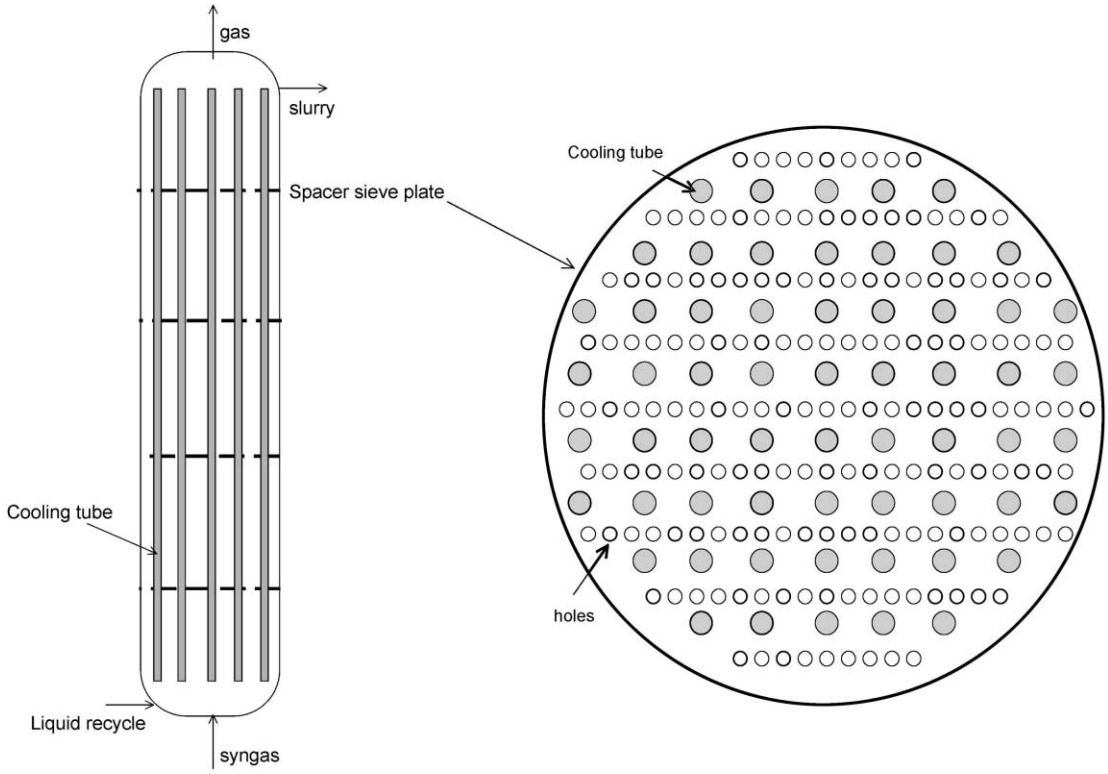

Fig. 1. Schematic of multi-stage bubble column slurry reactor.

is influenced by system properties, pressure, solids concentration and column size [1–3,13–35].

Due to the high rise velocity of the large bubbles (1–2 m s^{-1}), we can reasonably assume plug flow conditions for the dilute phase. Therefore, the upward motion of the large bubbles churns up the dense phase causing a certain degree of slurry backmixing, which guarantees good catalyst dispersion. The extent of dense phase backmixing depends on many factors: reactor geometry (aspect ratio), internal configuration and superficial gas (and eventually liquid) velocity. In large-scale reactors (5–10 m diameter, up to 30 m tall) equipped with longitudinal cooling tubes, the dense phase is fairly well mixed [10]. In order to decrease the reaction volume, or increase the reactor productivity, it is advantageous to have plug flow conditions of both the dilute and the dense phase (i.e. the liquid phase). To realise a plug flow regime of the dense phase, we have investigated the influence of staging the bubble column slurry reactor. Staging is achieved introducing intermediate "baffles", which could be sieve plates, which also function as spacers for the cooling tubes. Adjusting the number of baffles, the "dense" phase could approach plug flow characteristics. In this case, due to the high exothermicity of the FT reaction, a temperature profile would be established along the reactor height. While a well-mixed dense phase allows operation at the highest temperature considered for the FT synthesis (depending on the hydrocarbon selectivity target), plug flow conditions limit the operation to a lower average temperature [10]. Fig. 2 compares the two extreme cases (well-mixed and plug flow conditions of the dense phase) for a commercial scale slurry bubble column reactor, with high syngas conversion per pass, where we set the maximum reactor temperature at 513 K. With a multi-stage reactor configuration, each stage is maintained at isothermal conditions and, by properly optimising the heat removal per stage, an optimal temperature profile could be obtained along the reactor height.

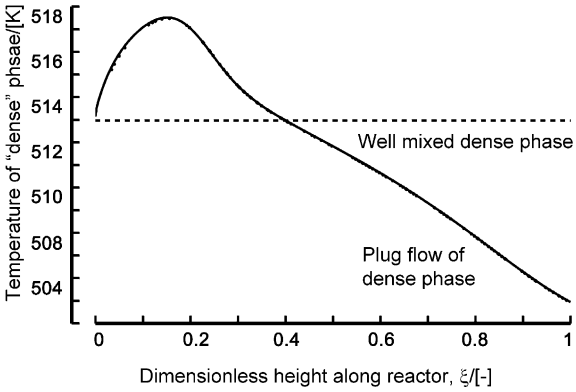

Fig. 2. Axial temperature profile for FT slurry bubble column: diameter, $D_T = 7\,m$; dispersion height, $H = 30\,m$; pressure, $P = 3\,MPa$; $\varepsilon_S = 0.35$; $T^{inlet} = 513\,K$; $U^{inlet} = 0.3\,m\,s^{-1}$; $a_w = 30.5\,m^2\,m^{-3}$.

3. Multi-stage reactor modelling

A multi-stage slurry reactor model has been developed for an FT industrial unit operating at 3 MPa and 513 K maximum temperature in the churn-turbulent regime. The column vessel has a diameter $D_T = 7\,m$, the total dispersion height is $H = 30\,m$, divided into N stages (with $N \geq 1$). The conceptual reactor model is depicted in Fig. 3. Within each stage, the dilute phase is in plug flow regime, the dense phase is completely mixed, isothermal conditions are maintained by means of internal cooling coils, and the catalyst particles, having an average size of 50 μm, are uniformly distributed within the dense phase.

The FT synthesis occurs according to the following simple scheme: $CO + 2H_2 \rightarrow -(CH_2)- + H_2O$, where $-(CH_2)-$ is the methylene group, which polymerises into a hydrocarbon chain. To describe the syngas consumption rate, we chose the intrinsic kinetic equation developed by Yates and Satterfield [36], which is a Langmuir–Hinshelwood type:

$$-R_{CO+H_2} = \frac{a p_{H_2} p_{CO}}{(1 + b p_{CO})^2} \quad (1)$$

Eq. (1) was based on experimental data obtained in a 1 l slurry autoclave with a cobalt-based catalyst (Co/MgO on SiO_2 support). This type of catalyst showed negligible water gas shift activity and the H_2/CO stoichiometric ratio can be reasonably

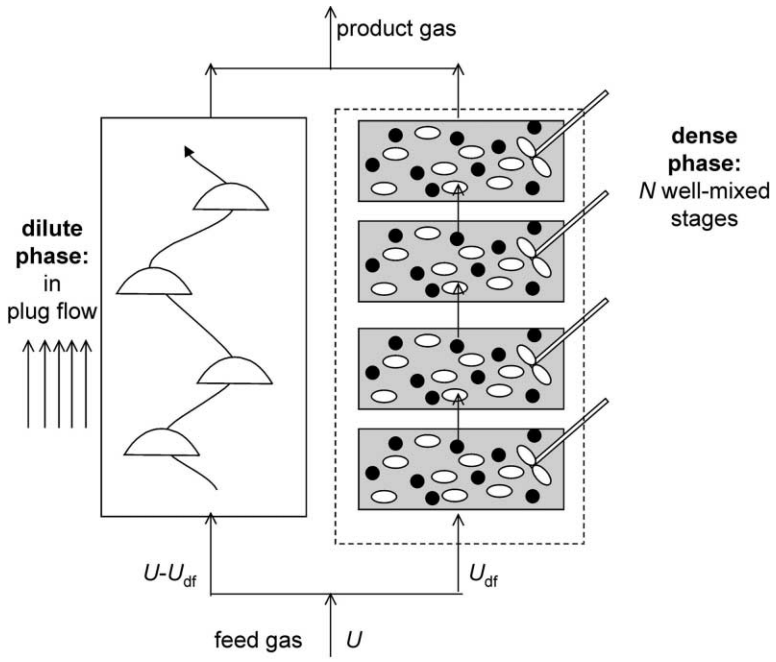

Fig. 3. Model of multi-stage bubble column reactor.

approximated to 2. The kinetic constant, a, and the absorption coefficient of species CO, b, are, respectively,

$$a = 8.8533 \times 10^{-3} \exp\left[4494.41\left(\frac{1}{493.15} - \frac{1}{T}\right)\right] \times (\text{mol kg}_{\text{cat}}\,\text{bar}^{-2}\,\text{s}^{-1}) \quad (2)$$

$$b = 2.226 \exp\left[-8236\left(\frac{1}{493.15} - \frac{1}{T}\right)\right] (\text{bar}^{-1}) \quad (3)$$

Catalyst selectivity was determined by means of the Anderson–Schultz–Flory mechanism for the carbon atom distribution: $x_n = (1 - \alpha_{\text{ASF}})\alpha_{\text{ASF}}^{n-1}$, where x_n is the molar fraction of the paraffin species C_nH_{2n+2} (considering negligible olefins and oxygenates content in the products), and α_{ASF} the Anderson–Shultz–Flory coefficient, i.e. the probability factor of hydrocarbon chain growth. In our simulations, we assumed $\alpha_{\text{ASF}} = 0.9$ [37], which corresponds to 70% middle distillates selectivity.

Previous studies demonstrated the advantage of working with slurry concentrations up to 40 vol.% [2,4]; so in our simulations of a multi-stage slurry reactor, we adopted a constant solids fraction, $\varepsilon_{\text{S}} = 0.35$. For such a concentrated slurry, the amount of gas entrapped in the dense phase as small bubbles can be neglected [17], that means all the gas phase passes through the column as large bubbles, hence in plug flow regime.

The volumetric mass transfer coefficient, $k_{\text{L}}a$, which is another important parameter affecting reactor performances [4], was determined by means of the following correlation:

$$\frac{(k_{\text{L}}a)_{\text{k}}}{\varepsilon} = \left(\frac{(k_{\text{L}}a)_{\text{k}}}{\varepsilon}\right)_{\text{ref}} \sqrt{\frac{D_{\text{L,k}}}{D_{\text{L,ref}}}} \quad (\text{k} = \text{CO}, \text{H}_2) \quad (4)$$

derived from the work of Vermeer and Krishna [38], who measured $k_{\text{L}}a$ for large bubbles in the churn-turbulent regime. The system studied was N_2–turpentine-5 and the data showed a constant value of the ratio $k_{\text{L}}a/\varepsilon_{\text{large}} = 0.5\,\text{s}^{-1}$. Since at our operating conditions $\varepsilon_{\text{large}} \approx \varepsilon$, hence we assumed $(k_{\text{L}}a/\varepsilon)_{\text{ref}} \approx k_{\text{L}}a/\varepsilon_{\text{large}} = 0.5\,\text{s}^{-1}$, and we predicted the volumetric mass transfer coefficient for different systems by means of the diffusion coefficient terms, as reported in Eq. (4), with $D_{\text{L,ref}} = 2 \times 10^{-9}\,\text{m}^2\,\text{s}^{-1}$. The diffusivities of H_2 and CO at 240°C are, respectively, 45.5×10^{-9} and $17.2 \times 10^{-9}\,\text{m}^2\,\text{s}^{-1}$.

The gas and liquid phase mass balances, which are solved for each stage, are the following.

Gas phase:

$$-\frac{\text{d}}{\text{d}z}(Uc_{\text{G,CO}}) - (k_{\text{L}}a)_{\text{CO}}\left(\frac{c_{\text{G,CO}}}{m_{\text{CO}}} - c^j_{\text{L,CO}}\right) = 0 \quad (5)$$

$$-\frac{\text{d}}{\text{d}z}(Uc_{\text{G,H}_2}) - (k_{\text{L}}a)_{\text{H}_2}\left(\frac{c_{\text{G,H}_2}}{m_{\text{H}_2}} - c^j_{\text{L,H}_2}\right) = 0 \quad (6)$$

Liquid phase:

$$A\int_{z_{j-1}}^{z_j} (k_{\text{L}}a)_{\text{CO}}\left(\frac{c_{\text{G,CO}}}{m_{\text{CO}}} - c^j_{\text{L,CO}}\right)\text{d}z + A(U_{\text{L}}^{j-1} - U_{\text{L}}^{j})c^j_{\text{L,CO}} - AH_N\varepsilon_{\text{L}}\frac{a^* c^j_{\text{L,CO}} c^j_{\text{L,H}_2}}{(1 + b^* c^j_{\text{L,CO}})^2} = 0 \quad (7)$$

$$A\int_{z_{j-1}}^{z_j} (k_{\text{L}}a)_{\text{H}_2}\left(\frac{c_{\text{G,H}_2}}{m_{\text{H}_2}} - c^j_{\text{L,H}_2}\right)\text{d}z + A(U_{\text{L}}^{j-1} - U_{\text{L}}^{j})c^j_{\text{L,H}_2} - 2AH_N\varepsilon_{\text{L}}\frac{a^* c^j_{\text{L,CO}} c^j_{\text{L,H}_2}}{(1 + b^* c^j_{\text{L,CO}})^2} = 0 \quad (8)$$

ε_{L} is the slurry holdup defined as $\varepsilon_{\text{L}} = 1 - \varepsilon$. The parameters m_{CO} and m_{H_2} are the solubilities of CO and H_2 defined by $c_{\text{G}} = mc^*_{\text{L}}$. Estimated values of these solubilities in the paraffin $C_{16}H_{34}$ (taken as FT liquid phase for properties evaluation), at a temperature of 240°C, are $m_{\text{CO}} = 2.48$ and $m_{\text{H}_2} = 2.96$. As the CO/H_2 feed ratio was set equal to the CO/H_2 consumption ratio (which is 2), the conversion of CO and H_2 are both equal to one another, and to the syngas conversion, $\chi_{\text{CO+H}_2}$. The model considers that resistance to mass transfer between the liquid phase and the catalyst surface, and intraparticle diffusion resistance are negligible; this assumption is valid due to the chosen particle size (50 μm). The contraction of gas volume, due to gaseous reagents consumption, was taken into account according to

$$U = U^{\text{inlet}}(1 + \alpha\chi_{\text{CO+H}_2}) \quad (9)$$

where the contraction factor α (for 100% syngas conversion) was estimated as $\alpha = -0.648$, assuming a 5 vol.% of inert content in the syngas. The set

of model equations represented by Eqs. (5)–(9) was implemented in a FORTRAN code.

The heat transfer coefficient from slurry to the coolant was estimated using the correlation of Deckwer et al. [39]:

$$St = 0.1(Re\,Fr_G\,Pr^2) \tag{10}$$

The slurry density is calculated from:

$$\rho_{SL} = \rho_L\left(1 - \frac{\rho_L}{\rho_{SK}}\varepsilon_S\right) + \rho_p\varepsilon_S \tag{11}$$

where ρ_p is the catalyst particle density (kg of solids m^{-3} of particle including voids), while ρ_{SK} the catalyst skeleton density (kg of solids m^{-3} of solids without voids). The void space within the particles are assumed to be completely filled with liquid. In order to determine the slurry viscosity, we use the modified Einstein's equation:

$$\mu_{SL} = \mu_L(1 + 4.5\varepsilon_S) \tag{12}$$

We assume that all the correlations to determine the model parameters are not affected by the presence of partition plates within the column. This means that the correlations are applicable to each stage. The gas holdup for each stage is determined on the basis of the superficial gas velocity prevailing in that stage. Each stage is assumed to be well mixed; this implies also that the temperatures and compositions are uniform on each stage.

4. Simulation results: effect of staging

We determined the effect of the number of stages performing simulations at different values of N (from 1 to 10) and changing the inlet superficial velocity from 0.1 to 0.4 m s^{-1}. The results, as regards syngas conversion and reactor productivity are reported in Figs. 4 and 5, respectively.

The advantage of a staging arrangement for the slurry phase is clearly evident. For example, operating at a superficial gas velocity of 0.3 m s^{-1} at the inlet, the syngas conversion increases from 0.88 to 0.96 when the stages increase from 1 to 4. Syngas conversion as a function of the number of stages, N, shows an asymptote, whose value depends on the operating conditions, hence on the superficial gas velocity. The asymptote

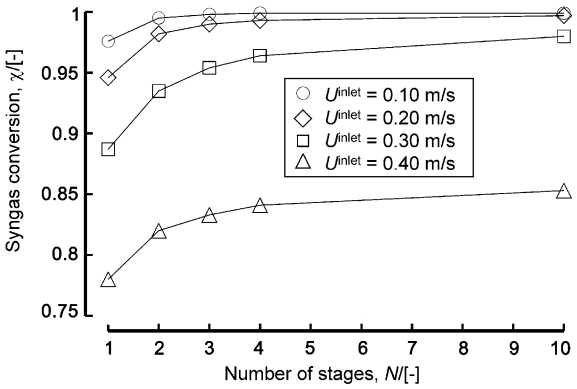

Fig. 4. Syngas conversion as a function of number of stages. FT slurry bubble column: diameter, $D_T = 7$ m; dispersion height, $H = 30$ m; pressure, $P = 3$ MPa; $\varepsilon_S = 0.35$; $T^{inlet} = 508.2$ K; $T_{max} = 513$ K; $a_w = 32\ m^2\ m^{-3}$.

corresponds to syngas conversion at which ideal plug flow conditions of the dense phase are assumed in the slurry bubble column reactor. Therefore, increasing N the dense phase approaches the plug flow regime. It is evident from Fig. 4 that there are no significant benefits from the slurry phase staging beyond 4. This means that, for the design of the FT multi-stage slurry bubble column reactor, four well-mixed compartments are sufficient. The inlet superficial gas velocity, U^{inlet}, is also an important design parameter. To reach high conversions per pass (>0.95) in the slurry bubble column without staging ($N = 1$), inlet superficial

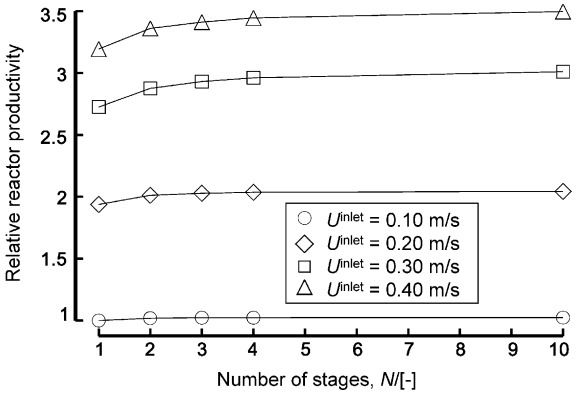

Fig. 5. Reactor productivity as a function of number of stages. FT slurry bubble column: diameter, $D_T = 7$ m; dispersion height, $H = 30$ m; pressure, $P = 3$ MPa; $\varepsilon_S = 0.35$; $T^{inlet} = 508.2$ K; $T_{max} = 513$ K; $a_w = 32\ m^2\ m^{-3}$.

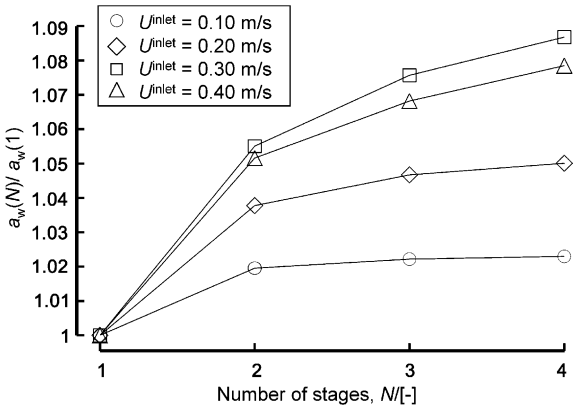

Fig. 6. Cooling tube specific surface area requirements.

gas velocities have to be lower than $0.2\,m\,s^{-1}$, limiting reactor productivity (see Fig. 5). Introducing the stages allows an increase of both syngas conversion and reactor productivity. Taking $U^{inlet} = 0.1\,m\,s^{-1}$ and $N = 1$ as the base case, we note that, increasing the stages and the superficial gas velocity, a significant increase of the reactor productivity is observed (see Fig. 5). However, to obtain conversion levels greater than say 0.95, with $N = 4$, we need to restrict the inlet superficial gas velocity to less than $0.3\,m\,s^{-1}$, the other operating conditions remaining the same (see Fig. 4).

The required specific heat transfer area of the cooling tubes, a_w, increases with the number of stages, since the productivity as well as reaction duty have increased. This is illustrated in the calculations shown in Fig. 6, where the variation of a_w, compared to the case without stages ($N = 1$), as a function of N and U^{inlet} is reported. The ratio $a_w(N)/a_w(1)$ is higher for $U^{inlet} = 0.3\,m\,s^{-1}$, compared to the case $U^{inlet} = 0.4\,m\,s^{-1}$. This is because for even though for $U^{inlet} = 0.4\,m\,s^{-1}$, the reactor productivity is the highest (see Fig. 5), the reactor conversion is lower than for the $0.3\,m\,s^{-1}$ case (see Fig. 4). The decrease in conversion with increasing gas velocity is an overriding factor in the determination of $a_w(N)/a_w(1)$. In order to maintain isothermal conditions within each stage and in the whole column, a_w has to be properly assigned to each compartment to remove all the heat of reaction locally produced. An example of a_w distribution is given in Table 1, in the case $U^{inlet} = 0.3\,m\,s^{-1}$.

In all our simulations, we imposed 10°C as temperature difference between the reactor and the coolant.

Table 1
Specific heat exchange surface area distribution within each compartment[a]

Position from the bottom	a_w (percentage fraction)			
	$N = 1$	$N = 2$	$N = 3$	$N = 4$
I	1	0.64	0.44	0.33
II	–	0.36	0.38	0.31
III	–	–	0.18	0.25
IV	–	–	–	0.11
Total	1	1	1	1
% increase of overall a_w with respect to base case of Fig. 6 ($N = 1$)	0	+5.5%	+7.5%	+8.7%

[a] N denotes the number of stages.

As shown from the data of Table 1, the bottom compartment, where syngas enters the reactor, requires the larger fraction of a_w, since the heat produced in the first stage is greater compared to the remaining stages, because of the higher partial pressures of the reactants.

5. Conclusions

Our simulation studies have shown that, dividing the bubble column slurry reactor into say 4 or more compartments, by means of sieve trays or other means, allows to approach plug flow conditions of both the dilute and dense phases. The solid catalyst in each stage is uniformly suspended, due to the well-mixed liquid phase within each stage and isothermal conditions are maintained within each stage. The multi-stage design results in significant improvements in both syngas conversion and reactor productivity, as compared to a well-mixed slurry reactor. In order to achieve high conversion levels (say above 0.95) without sacrificing the productivity, the inlet superficial gas velocity has to be limited to about $0.3\,m\,s^{-1}$. However, additional cooling tubes need to be installed.

References

[1] J.W.A. de Swart, R. Krishna, S.T. Sie, Stud. Surf. Sci. Catal. 107 (1997) 213.
[2] R. Krishna, C. Maretto, Stud. Surf. Sci. Catal. 119 (1998) 197.
[3] R. Krishna, J. Ellenberger, S.T. Sie, Chem. Eng. Sci. 51 (1996) 2041.

[4] C. Maretto, R. Krishna, Catal. Today 52 (1999) 279.
[5] G.P. Van der Laan, A.A.C.M. Beenackers, R. Krishna, Chem. Eng. Sci. 54 (1999) 5013.
[6] S.T. Sie, R. Krishna, Appl. Catal. A 186 (1999) 55.
[7] R. Krishna, S.T. Sie, Fuel Process. Technol. 64 (2000) 73.
[8] R. Krishna, Oil Gas Sci. Technol. 55 (2000) 359.
[9] B. Jager, Stud. Surf. Sci. Catal. 119 (1998) 943.
[10] R.L. Espinoza, A.P. Steynberg, B. Jager, A.C. Vosloo, Appl. Catal. A 186 (1999) 13.
[11] B. Eisenberg, R.A. Fiato, C.H. Mauldin, G.R. Say, S.L. Soled, Stud. Surf. Sci. Catal. 119 (1998) 943.
[12] B. Eisenberg, R.A. Fiato, T.G. Kaufmann, R.F. Bauman, Chemtech 10 (1999) 32.
[13] J. Ellenberger, R. Krishna, Chem. Eng. Sci. 49 (1994) 5391.
[14] J.W.A. de Swart, R. Krishna, Chem. Eng. Res. Des., Trans. Inst. Chem. Engrs. 73 (1995) 308.
[15] J.W.A. de Swart, R.E. van Vliet, R. Krishna, Chem. Eng. Sci. 51 (1996) 4619.
[16] R. Krishna, J. Ellenberger, AIChE J. 42 (1996) 2627.
[17] R. Krishna, J.W.A. de Swart, J. Ellenberger, G.B. Martina, C. Maretto, AIChE J. 43 (1997) 311.
[18] H.M. Letzel, J.C. Schouten, C.M. van den Bleek, R. Krishna, Chem. Eng. Sci. 52 (1997) 3733.
[19] H.M. Letzel, J.C. Schouten, R. Krishna, C.M. van den Bleek, Chem. Eng. Sci. 52 (1997) 4447.
[20] M.H. Letzel, J.C. Schouten, C.M. van den Bleek, R. Krishna, AIChE J. 44 (1998) 2333.
[21] R. Krishna, J.M. van Baten, J. Ellenberger, Powder Technol. 100 (1998) 137.
[22] R. Krishna, M.I. Urseanu, J.M. van Baten, J. Ellenberger, Chem. Eng. Sci. 54 (1999) 171.
[23] R. Krishna, J.M. van Baten, Nature 398 (1999) 208.
[24] H.M. Letzel, J.C. Schouten, C.M. van den Bleek, R. Krishna, Chem. Eng. Sci. 54 (1999) 2237.
[25] R. Krishna, M.I. Urseanu, J.M. van Baten, J. Ellenberger, Chem. Eng. Sci. 54 (1999) 4903.
[26] R. Krishna, J.M. van Baten, J. Ellenberger, A.P. Higler, R. Taylor, Chem. Eng. Res. Des., Trans. Inst. Chem. Engrs. 77 (1999) 639.
[27] R. Krishna, M.I. Urseanu, J.M. van Baten, J. Ellenberger, Int. Commun. Heat Mass Transfer 26 (1999) 781.
[28] R. Krishna, J.M. van Baten, Int. Commun. Heat Mass Transfer 26 (1999) 965.
[29] J.M. van Baten, R. Krishna, Chem. Eng. J. 77 (2000) 143.
[30] R. Krishna, M.I. Urseanu, A.J. Dreher, Chem. Eng. Process. 39 (2000) 371.
[31] R. Krishna, J.M. van Baten, M.I. Urseanu, Chem. Eng. Sci. 55 (2000) 3275.
[32] R. Krishna, J.M. van Baten, M.I. Urseanu, J. Ellenberger, Chem. Eng. Process. 39 (2000) 433.
[33] R. Krishna, M.I. Urseanu, J.M. van Baten, J. Ellenberger, Chem. Eng. J. 78 (2000) 43.
[34] R. Krishna, M.I. Urseanu, J.W.A. de Swart, J. Ellenberger, Can. J. Chem. Eng. 78 (2000) 442.
[35] R. Krishna, A.J. Dreher, M.I. Urseanu, Int. Commun. Heat Mass Transfer 27 (2000) 465.
[36] I.C. Yates, C.N. Satterfield, Energy and Fuels 5 (1991) 168.
[37] I.C. Yates, C.C. Chanenchuk, C.N. Satterfield, DOE Report No. PC79816-6, Contract No. DE-AC22-87PC79816, July–September 1989.
[38] D.J. Vermeer, R. Krishna, Ind. Eng. Chem. Process. Des. Dev. 20 (1981) 475.
[39] W.D. Deckwer, Y. Serpemen, M. Ralek, B. Schmidt, Ind. Eng. Chem. Process. Des. Dev. 21 (1982) 231.